GRANT

IN-45-CR

72167

P-50

SECOND SEMIANNUAL PROGRESS REPORT

TO: NATIONAL AERONAUTICS AND SPACE ADMINISTRATION

FROM: NORTH CAROLINA STATE UNIVERSITY, RALEIGH, NC 27695

FOR: **"HETEROGENEOUS PHOTOCATALYTIC OXIDATION OF ATMOSPHERIC TRACE CONTAMINANTS" (NAG 2-684)**

BY: DAVID F. OLLIS AND JOSE PERAL
CHEMICAL ENGINEERING DEPARTMENT
NORTH CAROLINA STATE UNIVERSITY
RALEIGH, NC 27695
PHONE: (919)-737-2329
FAX: (919) 737-3465

PERIOD COVERED: 5/1/91 THROUGH 11/1/91

PRINCIPAL INVESTIGATOR:

DAVID F. OLLIS, PROFESSOR

SUBMITTED: 2/7/92

SUMMARY:

A two year study to examine the feasibility of using heterogeneous photocatalysis for spacecraft air purification was begun at NCSU on November, 1, 1990. The original grant proposal included examination of the rates of destruction of anticipated spacecraft generated air contaminants, including alcohols, aldehydes, chlorinated compounds,as well as trace levels of volatile compounds containing nitrogen, sulfur, and silicon.

In the second six month period of 5/1/91-11/1/91, the following items were demonstrated or accomplished:

(1) initiation of research effort of Mr. Michael Sauer, PhD candidate. Michael will construct a *recirculating photoreactor* and carry out an engineering analysis of it in order to allow simulation and experimental validation of an enclosed air treatment system. His research plan is the attached p. 1.

(2) initiation of research effort of Ms. Yang Luo, PhD candidate. Ms. Luo will construct and carry out an engineering analysis of a one or more *logical catalyst configurations* in order to establish a design basis for heterogeneous photoreactors for air treatment. Her research plan is the attached p. 2

(3) completed and submitted a paper "*Heterogeneous Photocatalytic Oxidation of Gas-Phase Organics for Air Purification*"by Dr. J. Peral and Prof. Ollis (Journal of Catalysis) A copy of this ms. is found in pp. 3 et seq. of attachment.

(4) completed a draft review of the entire gas-solid photo-catalyst literature for oxidation (Peral and Ollis); copy of final version to accompany next semiannual report.

(5) initiated experimental study of photocatalytic destruction of air contaminants capable of solid product deposition (siloxane for silicate, indole for nitrate, etc) As destruction of all major contaminant classes has now been demonstrated, proof of catalyst lifetime/deactivation rate is now needed.

(6) Presentations of NASA sponsored grant results were made at the following locations (same paper in all cases)

AIChE meeting, Pittsburgh, PA, August, 1991

NASA Langley, Hampton VA, October 1991

Exxon Frontiers in Catalysis Meeting, Annandale, NJ, November, 1991.

Future presentation at ACS meeting, San Francisco, April, 1992.

The third six month period will include initial calculations of fundamental kinetic and fluid mechanical modelling of flow and reaction in a fixed bed photocatalyst (Luo), completion of the catalyst deposition studies (Peral), and a detailed plan of work for Sauer in completing the recirculating photoreactor assembly , testing, and operation..

10/24/91

Research Program: Michael Sauer, Research Assistant: NASA Grant

PROPOSED SCHEDULE: Multicomponent conversion in a recirculating batch air chamber

1. Chamber system design	8-9/91
2. Chamber system assembly	10/91
3. Initial operation and testing	11-12/91
4. Simulated atmosphere batch runs	
(a) single component calibrations	1/92
(b) dual component runs	2-3/92
(c) ternary runs	4-5/92
(d) complete simulated atmosphere runs	6-7/92
(e) water variation influences	8/92
(f) reactor analysis	9/92
5. Research proposition (NCSU) submitted	9/92
6. NASA draft report	10/92
7. FINAL report	11/92

10/17/91

Research plan for Ms. Yang Luo: NASA grant research assistant

1. Reactor modelling:

   Flow and concentration field equations 8/91

   Numerical programming of solution techniques 11/91

2. Design of catalyst chamber for fundamental flow and conversion studies 1/92

3. Research proposal (dept.) presented 1/92

4. Assembly of flow reactor 2/92

5. Flow and illumination vs. performance studies 3-9/92

6. Report writing: Fundamental reactor analysis and experimental results 10/92

7. FINAL report(draft) to NASA 11/92

D. Ollis
10/91

HETEROGENEOUS PHOTOCATALYTIC OXIDATION OF GAS-PHASE ORGANICS FOR AIR PURIFICATION: ACETONE, 1-BUTANOL, BUTYRALDEHYDE, FORMALDEHYDE and m-XYLENE OXIDATION

José Peral and David F. Ollis

Department of Chemical Engineering, North Carolina State University, Raleigh, North Carolina 27695-7905

Submitted to: Journal of Catalysis

SUMMARY

Photocatalyzed degradations of various trace oxygenates and an aromatic in air were carried out using near-UV illuminated titanium dioxide (anatase) powder. Feed concentrations of these prototypical contaminants for a steady state flow reactor were in the range 0-260 ppm in all runs. The initial rates of degradation for acetone, 1-butanol, formaldehyde and m-xylene were well described by simple Langmuir-Hinshelwood rate forms. No reaction intermediates were detected for acetone oxidation at conversions of 5-20 %. Butyraldehyde was the main product of 1-butanol oxidation for conversions of 20-30 %. The influence of 5 % water (simulating partial humidification) in the feedstream varied strongly: water vapor inhibited acetone oxidation, but had no influence on 1-butanol conversion rate. Some catalyst deactivation was detected between 1-butanol runs after the reactor was maintained in the dark in the presence of 1-butanol; the activity could be easily recovered by illuminating the catalyst in fresh air. Formaldehyde was also succesfully oxidized. These results taken together with earlier literature citations for photocatalyzed total oxidation of methane, ethane, trichloroethylene, toluene, and a very recent report for oxidation of odor compounds indicate a favorable technical potential for photocatalyzed treatment of air in order to degrade and remove all major classes of oxidizable air contaminants.

INTRODUCTION

The removal of undesired organic contaminants in air has been a topic of major and continuing emphasis over the last decade. Potential application sites for air purification and decontamination technologies include completely or partially enclosed atmospheres such as are found in spacecraft, office buildings, factories and homes. As a large number of the common air contaminants of concern are oxidizable, the need for an oxidative destruction process is self-evident. Heterogeneous catalytic oxidation technology for gas phase pollution control has well established examples in automotive exhaust and catalytic incineration. However, nearly all heterogeneous oxidation catalysts function at elevated temperatures, whereas nearly all inhabited atmospheres of concern to man exist at or near 20-25 °C. Further, a need exists for an air purification catalyst which can not only function at ambient conditions of temperature and pressure, but which can also use the mildest and most prevalent oxidant, molecular oxygen (O_2), and which is active against the broadest possible range of contaminant structures.

One oxidation catalyst candidate which operates at room temperature using molecular oxygen is a photocatalyst. Heterogeneous photocatalysis is the name of the ambient temperature process in which the surface of an illuminated semiconductor acts as a chemical reaction catalyst by using bandgap light as a source of solid excitation. These semiconductor compounds usually have a moderate energy bandgap (1-3.7 eV) between their valence and conduction bands. Under illumination with photons of bandgap or greater energy, the valence band electrons are photo-excited into the conduction band, creating highly reactive

electron hole-pairs which, after migrating to the solid surface, may participate in charge-transfer reactions with adsorbates and provoke the reduction or oxidation of such species.

Most of the heterogeneous photocatalysis reports of the last decade have dealt with aqueous solutions, exploring water decontamination and purification by the photoassisted oxidative destruction of hazardous solutes (1-3).

Studies involving gas-phase heterogeneous photocatalysis are far fewer, but the modest existing literature has demonstrated that near-UV illumination in concert with anatase titanium dioxide (TiO_2) photocatalyst and molecular oxygen can carry out the complete oxidation of several small hydrocarbons (methane and ethane) (4), an aromatic (toluene) (5), a halocarbon (trichloroethylene (TCE)) (6), and carbon monoxide (4). The heterogeneous photo-oxidations of some of the organics examined out in the present paper have been previously reported by other authors using much higher reactant concentrations: Blake and Griffin studied 1-butanol heterogeneous photo-oxidation for 1:21 molar ratios of butanol:oxygen (7) and Stone et al. reported photo-oxidized acetone at 10 % concentration in an O_2 atmosphere (8). Finally, in a very recent paper received by us while preparing this paper, Suzuki et al (9) reported use of inmobilized TiO_2 for photocatalytic air deodorization. Their brief (2 pages) paper presented evidence for photocatalyzed oxidation of acetaldehyde, isobutyric acid, toluene, methylmercaptan, hydrogen sulfide, and trimethylamine. They reported only a single run for each reactant (with initial concentrations between 5-80 ppm) and suggested that the variation of reactant with time was first order.

The present gas-solid photocatalysis study was undertaken for two reasons:
(i) A survey of the literature on spacecraft, office, building and factory air quality indicates that a central class of offending chemicals are oxygenates, e.g., aldehydes, ketones and alcohols. Accordingly, we have initiated and report here an examination of the photocatalytic destruction of formaldehyde, butyraldehyde, acetone and 1-butanol.
(ii) With the exception of the toluene (5), TCE (6) and Suzuki (9) reports, all prior studies were for organic vapor phase concentrations much higher than the 1-500 ppm (mass) characteristic of short term exposure standards or odor threshold levels. Accordingly we wished to explore oxygenate conversion kinetics at the very low contaminant pressures appropriate to lightly contaminated air at one atmosphere.

As application to air treatment in habitable atmospheres is our focus, we also examined the importance of relative humidity on observed rates, as Ibusuki et al (5) and Dibble and Raupp (6) have each noted a strong influence of water concentration in the range of conventional air humidification.

EXPERIMENTAL

Figure 1 shows an schematic of the flow reactor experimental system used for the photo-oxidation studies. UHP air tank (Linde) was used to bring a 20.11 l gas reservoir to one atmosphere. A suitable amount of contaminant in liquid form was then injected into the reservoir through a sample port. Following vaporization (the final reactant pressure was in all cases lower than the pure liquid vapor pressure), the reservoir is then filled with additional air up to a final desired pressure (typically $2.18 \cdot 10^5$ N/m^2) which was sufficient to provide the desired gas flow rates over periods up to several hours. An air stream from the tank and a gas mixture stream from this lightly pressurized reservoir were continuously mixed, and passed to the reactor through mass flow sensor-controllers coupled to a mass flow controller unit (Linde FM4574). A wide range of contaminant feed concentrations could be examined for flow reactor studies by variation of the two stream rates relative to each other.

The photoreactor was a cylindrical vessel (4 cm high and 3.14 cm^2 base) with an interior, attached fritted glass plate used to support the powdered photocatalyst and through which the downward flow passed. An air-tight quartz window enclosed the reactor top. Two lateral ports provided the inlet and outlet for the gas mixture, and a thermocouple (always in the dark) was installed just downstream of the glass frit. The photo-excitation light source was placed directly above the reactor window.

A gas sampling loop allowed capture of aliquots of either the reactant feed or the product stream; a reactor bypass allowed the direct flow of the reactant

mixture to the sampling loop. Except with formaldehyde feeds, all vapor samples were analyzed by gas chromatography (Perkin Elmer Sigma 1) operating with a flame ionization detector (FID). Formaldehyde analysis was performed by first passing the reactor product gas stream through adsorption tubes containing N-benzylethanolamine (Supelco ORBO 22 tubes); this chemical reacted with formaldehyde to form 3-benzyloxazolidine (10) which in turn could be analyzed by capillary gas chromatography. For GC-MS identification analysis, samples were first concentrated by passing the reactor exhaust through charcoal tubes, and subsequently extracting and diluting the adsorbate content in a suitable organic solvent. A Hewlett-Packard 5985B was used for these measurements.

The catalyst used was P25 TiO_2 (Degussa). According to the manufacturer the primary particle diameter was 30 nm with a surface area of 50±15 m^2/g, and the crystal structure was primarily anatase. The P25 particles were spherical and nonporous, with a stated purity of >99.5% TiO_2 . Stated impurities included: Al_2O_3 (<0.3%), HCl (<0.3%), SiO_2 (<0.2%), and Fe_2O_3 (<0.01%). This powdered semiconductor catalyst was used as supplied without any pretreatment. The acetone, 1-butanol and butyraldehyde used to prepare individual gas mixtures were of HPLC grade, supplied by Aldrich. The formaldehyde source was a 37% (W/W) aqueous solution containing 10-15 % methanol as a stabilizer.

Either of two light sources were used: a 200 W high pressure Hg-Xe lamp (Oriel Corp.) or a 100 W blacklight (UVP). To prevent any true UV (200-300 nm) homogeneous photoreaction, a Pyrex plate was positioned over the reactor window to absorb the incident radiation having λ<300 nm and to transmit only the near-UV light for the TiO_2 photoactivation. Neutral screens were used for the intensity

variation studies, and the resultant incident light fluxes were measured with ferrioxalate liquid actinometers placed under the quartz-reactor window. In a typical experiment, 0.1 g of TiO_2 powder was spread uniformly over the surface of the porous fritted glass plate, providing a 3.2 mm TiO_2 powder layer. Both the catalyst and the fritted glass had appreciable surface areas. For the previous photocatalyst partial oxidation studies, which involved reactant partial pressures of 0.1 to several atmospheres, these surfaces would have been expected to come rapidly to a gas-solid equilibrium in a flow reactor. With our only slightly contaminated air feed, however, the surface inventory of strongly held reactant required some time to accumulate to a "dark" gas-solid equilibrium. Consequently, the trace contaminated air had first to be fed for a considerable period of time (typically 60-90 min) until the feed and reactor exit gas concentrations were identical (no "dark" reaction products were noted). When that condition was achieved, the light was turned on, and gas samples were taken every 10-20 min. The irradiation was maintained for a convenient period of time (2-6 hours) to establish that the photo-steady-state was achieved. Gas flow rates of 70-120 ml/min were used through the experiments, providing reaction rates which were esentially free of mass transfer influences, as shown by calculation of the mass transfer coefficient in packed bed reactors (11) (see appendix).

RESULTS

Acetone photo-oxidation

Gas-phase acetone photo-oxidation over TiO_2 rutile has been previously reported by Stone et al. (8). These authors carried out the batch oxidation of one monolayer of acetone in O_2 atmosphere and found formation of formaldehyde and CO at only trace levels, with CO_2 and water as the major and final conversion products. Teichner et al (12) found acetone to be the only major intermediate of the photocatalytic oxidation of isobutane under hydrocarbon rich conditions. No subsequent organic intermediates were reported, and these authors showed that acetone and other organics yielded CO_2 as the final photo-oxidation products over TiO_2 (13). In contrast to these earlier studies, our experiments used very low acetone gas phase concentrations (75-250 mg/m^3). Dark acetone gas mixture flows over the TiO_2 showed a moderate equilibrated extent of acetone adsorption (0.206 mg acetone/100 mg TiO_2), corresponding to an initial surface coverage of 0.85 acetone molecules per nm^2.

Under illumination, a substantial decrease of the acetone exit concentration was noticed, and no oxidizable products of reaction were found by FID. Formaldehyde, if formed, has a very small heat of combustion which would have prevented its FID detection.

The steady-state acetone inlet and outlet concentrations are shown in Table 1. Conversions of 15-20% were achieved under the reported experimental conditions. As the activity of the illuminated catalyst was sufficient to provide

appreciable conversion of acetone, we consider a simple plug flow integral analysis of the data in order to describe the change of acetone concentration through the illuminated outermost TiO_2 layer where light absorption takes place. The reaction rate constant will vary with intensity I as I^{α} with α=1 at very low intensities (14,15) and α=0.5 at very high values (13,16). Over the single decade variation in irradiance used here, the reaction rate constant will depend on the intensity of light at any depth and on the value of the exponent α (taken to be constant):

$$k = k_0\left(\frac{I}{I_0}\right)^{\alpha} = k_0 e^{-\alpha\epsilon z} \qquad (1)$$

wher ϵ is the effective adsorption coefficient of TiO_2.

Langmuir-Hinshelwood (LH) rate forms have been widely used in liquid phase photocatalysis, and have been found of utility in gas phase TCE destruction (6) and alkane partial oxidation (17). Assuming an L-H form for the present systems, plug flow through our thin packed bed gives:

$$v\frac{dC}{dz} = -\frac{kKC}{1+KC} = -\frac{k_0 e^{-\alpha\epsilon z}KC}{1+KC} \qquad (2)$$

where v is the gas linear velocity, C the gas phase concentration of acetone, and z the axial coordinate through the TiO_2 layer. Integration of equation (2), assuming complete light absorption, and rearrangement gives eq (3):

$$\frac{\ln\frac{C}{C_0}}{C-C_0} = -\frac{k_0 K}{\alpha\epsilon z}\frac{1}{C-C_0} - K \qquad (3)$$

If the assumed L-H form is valid, then a plot of $(C-C_0)^{-1}\cdot\ln(C/C^0)$ vs. $(C-C_0)^{-1}$ should be linear, with a negative slope $-k_0K/(\alpha\epsilon v)$ and a y-axis intercept at $(C-C_0)^{-1}\cdot\ln(C/C_0) = -K$. Figure 2 indicates that the experimental data is in good agreement with this integral rate-law analysis. Values of k and K can be calculated if the TiO_2 absorption coefficient ϵ and the exponent α are previously known. As reported by Teichner et al. (4), 99 % of light absorption (optical density=2) occurs within a TiO_2 anatase layer of 4.5 μm, and so an ϵ value of 10211 cm^{-1} can be estimated. Values of k=7.75 g/l·min and K=0.00644 m^3/mg were found from the intercept and slope in figure 2, when α=0.7 as found below.

The photocatalyzed oxidation rate was expected to be intensity dependent as reflected in prior literature. A plot of log acetone rate vs. log I_a (incident irradiation) gives a straight line of slope 0.7±0.1 (figure 3). Thus the reaction rate follows equation (4):

$$Rate = K' I_a^{0.7} f(reactant) \qquad (4)$$

This equation describes a transition regime (α=0.7) between the two asymptotic values reported above ($0.5 \le \alpha \le 1.0$).

In liquid phase systems the photocatalytic efficiency of utilization of light to drive the desired oxidation reaction is represented by the apparent quantum yield, q, defined by the equation q = molecules reacted/photons absorbed. This calculated apparent quantum yield is also plotted vs. irradiance in figure 3. For a process rate which is first order in irradiance, the quantum yield would be constant. For a half-order rate dependence on irradiance, the quantum yield would vary inversely with the square root of irradiance (-0.5 order). For the present

acetone oxidation, q varies as:

$$q \propto \frac{rate}{I_a'} \propto \frac{I_a^{0.7}}{I_a'} = I_a^{-0.3} \qquad (5)$$

Several authors have previously reported the need for traces of water (hydroxyl groups) on the TiO_2 surface in order to maintain vapor phase photocatalytic oxidation activity for extended periods of time (6,18). A prior TCE oxidation study (6) also noted strong water inhibition at the higher water levels used here. We observed that water in the gas feed inhibits the acetone oxidation rate. The dependence of rate on the water concentration may be described by the relationship:

$$r = \frac{r_0}{1 + K_H [H_2O]^a} \qquad (6)$$

where r_0 is the reaction rate free of water effect. Figure 4 shows that experimental data can be fitted by the equation $1/r = 1100 + 0.00106[H_2O]^{1.674}$, which is the inverse of equation (6):

$$\frac{1}{r} = \frac{1}{r_0} + \frac{K_H}{r_0} [H_2O]^a \qquad (7)$$

From this data fitting we obtain $a \approx 1.7$, $r_0 = 0.909$ μg/min·cm^2 and $K_H = 9.6 \cdot 10^{-7}$ m^3/mg.

1-Butanol photo-oxidation

For fresh catalyst in the dark, considerable time (2 hours) was required to achieve a reactor exit concentration equal to the feed value. The integrated ΔConcentration difference of flow over time indicated that 2.01 mg of 1-butanol

was adsorbed onto the catalyst (100 mg) and frit. This value indicates 10 times more mass adsorption for 1-butanol than for acetone, and corresponds to a surface coverage of 5.88 1-butanol molecules/nm^2 TiO_2. These results confirm a strong affinity between the alcohol and the metal oxide surface.

Under illumination, the 1-butanol steady-state exit concentration was decreased and two intermediate products peaks appeared (major, minor). It is well known that alcohol oxidation over metal oxide surfaces may take place through two different reaction pathways: the formation of an aldehyde (dehydrogenation reaction) or an olefin (dehydration reaction), each with the same number of carbons (19). Blake and Griffin (7) found both butyraldehyde and 1-butene to be formed during the photocatalyzed oxidation of 1-butanol over TiO_2 at much higher butanol/oxygen ratios (1 mol butanol/22 mol O_2) than used in our study. The largest of the two new peaks observed in the present study was verified as butyraldehyde by direct injection of this organic for its GC-FID detection. Attempts to associate the trace, second GC-peak with butene by direct injection of 1-butene were unsuccessful. Using the GC calibration curve of 1-butanol to estimate the amounts of the unknown intermediate, a simple mass balance on reactant converted and products formed indicated that some further oxidation of these intermediates had taken place, probably to CO_2.

Butyraldehyde heterogeneous photo-oxidation experiments were also carried out. A noticeable decrease of steady-state butyraldehyde exit concentration was observed when a gas mixture of 118 mg/m^3 of this reactant was continuously fed into the reactor. A steady-state reaction rate of 1.5 $\mu g/cm^2 \cdot min$ was achieved after 150 min. A secondary GC-peak was observed, with retention time identical

to that of the unknown detected during 1-butanol photo-oxidation. That peak may thus correspond to a product of butyraldehyde oxidation rather, than the suspected 1-butene formed through dehydration of 1-butanol.

Table I summarized the steady state concentrations of 1-butanol in the gas stream entering and leaving the photochemical reactor. The rates calculated from this data can be fitted by using the integral L-H rate form developed above (figure 5). The apparent rate and binding constants of 1-butanol are k=49.2 g/l·min and K=0.00109 m^3/mg, respectively.

Figure 6 indicates that variations in water vapor content have no significant effect on the rate of disappearance of 1-butanol. A very slight decline of conversion is noticed in the data, and the concentration of butyraldehyde formed is also seen to be unaffected by the water vapor content.

Photocatalyst Deactivation

In a typical 1-butanol photo-oxidation experiment, commencement of illumination produced a very high initial disappearance rate of 1-butanol and a rapid rise in appearance of butyraldehyde. With time, 1-butanol conversion decreased markedly, and reached steady-state conditions of about 30% conversion in 100 minutes. Following a subsequent dark period of 200 minutes, during which reactant gas flow was halted, illumination again resulted in achievement of a steady-state 1-butanol photo-oxidation but with lower conversions (18-19%), as seen in figure 7. Thus, a transient catalyst deactivation took place during the time just after

each dark period. A subsequent dark period and reillumination again produced a deactivation to a new steady-state with still lower conversion. The butyraldehyde formation rate also decreased after dark and re-illumination periods. At these eventual steady-states, the 1-butanol consumed equalled the butyraldehyde produced, and the concentration of the unknown second product was virtually zero. This behaviour was found in a range of 1-butanol concentrations of 140-260 mg/m^3.

Verification that steady-state conditions were achieved was accomplished through "long term" illuminations of more than 6 hours, carried out in the presence of 1000 mg/m^3 water in the gas feed. When similar experiments were repeated in the a total absence of water in the feed, the loss of catalyst activity was continuous and no steady-state conditions were achieved. This latter continuous loss of activity is in agreement with the essential need of surface water for the occurrence of photoassisted oxidation over metal oxides as reported by others (6,20).

To regenerate catalyst activity following deactivation in 1-butanol experiments, a series of catalyst treatments were explored. The treatments along with the subsequent initial activities are summarized in Table 2. No recovery of photocatalytic activity was noticed when a pure air flow was passed through the reactor in dark conditions; even at 60-80 C°, the dark, pure air flow is insufficient for any recovery. However, replacement of contaminated air by pure air (with no water vapor) and continued illumination and flow for varying periods of time resulted in a progressive regeneration of catalyst activity, ultimately reaching to near the original level. This result indicates that some strongly

adsorbed, oxidizable intermediate or side products must be responsible for the photoactivity decay; the intermediate can in turn be photo-oxidized but at low rates compared with 1-butanol oxidation. As an aside, the first point in figure 5 was the first run performed for 1-butanol photo-oxidation; it shows a higher rate than later data would suggest. The remaining data describes a Langmuir-Hinshelwood behaviour with a partialy deactivated catalyst and no intervening dark periods.

Operations above ambient temperatures (61-62 °C or 75-80 °C) were examined. No noticeable rate differences were found with reaction temperature, and after each new dark period, deactivation again occurred to give lower steady-state 1-butanol conversions, with nearly exclusive butyraldehyde formation.

The same transient decay of photo-catalytic activity after dark periods was observed when photo-oxidizing butyraldehyde, which indicates that the species responsible for the deactivation may be the same in both cases.

Attempts to detect intermediate reaction products were made by means of GC-MS analysis. The organic species present in the reactor exhaust were retained over charcoal adsorption tubes and extracted with a suitable solvent before injection into the GC carrier gas stream. Some GC-peaks of retention times longer than for 1-butanol were obtained, corresponding to compounds of higher molecular weight. Because none of those peaks were noticed through direct gas sample GC injections, it may be assumed that the new products were formed by reactions between the charcoal-adsorbed species under dark conditions; a second, faint possibility would be formation over the TiO_2 but in such small amounts that only long time

charcoal tube sample collection provided detection. The peaks that could be identified belonged to chemical structures clearly related to 1-butanol, such as butyl esters of acetic, formic and propionic acids, dibutoxy methanol and the anhydride of butanoic acid.

When reactive gas samples of butyraldehyde were passed through the charcoal adsorption tubes without previous photoreaction, again peaks of compounds of higher molecular weight were obtained, indicating that the butyraldehyde is highly reactive in the adsorbed state. The products identified were 1-butanol, 2-buten-1-ol and butyl esters of propanoic and butanoic acids. After photocatalytic treatment and carbon tube collection of the reacted butyraldehyde gas samples, new peaks of higher molecular weight were detected, including butanoic acid, 2-ethylhexanal, the ethylester of propanoic acid, and 2-butanone.

Formaldehyde Photo-oxidation

Formaldehyde has been reported (8) to be a trace intermediate of acetone photo-oxidation and it may be expected to occur as an intermediate in the final steps of other organic oxidations. As formaldehyde is one of the more frequently detected pollutants in enclosed atmospheres, its elimination is of clear interest. In our preliminary experiments, high conversions of formaldehyde were obtained as shown in Table 1. The destruction of this pollutant at levels of 1 ppm, which corresponds to its threshold limit value-time weighted average (21), appears to be possible by heterogeneous photocatalysis. Figure 8 shows that most formaldehyde experimental data also fit the integrated L-H rate law; only the

point corresponding to an outlet flow estimated to have 0.1 ppm formaldehyde strongly deviates from the linearity suggested by other data. This may be due to our analytical limitations of about 1 ppm; we are currently exploring equipment modification to include a methane convertor that will improve our detection limits. Simultaneous photocatalytic oxidation of methanol, present as a formaldehyde solution stabilizer, was confirmed by means of direct GC-FID analysis. The high photocatalytic reactivity of formaldehyde, even in the joint presence of methanol, indicates that photocatalysis is a good candidate treatment for removal of trace formaldehyde from air.

The apparent high reactivity of formaldehyde (and methanol) is consistent with the finding by Suzuki et al (9) that photocatalyzed oxidation of another small oxygenate, acetaldehyde, proceeds so rapidly through any intermediates that none were detected and the molar ratio of CO_2 produced per acetaldehyde consumed was 2 at all conversions studied.

m-Xylene Photo-oxidation

As an example of trace level gas-phase photo-oxidation of aromatics compounds, we include here data of m-xylene oxidation. Ibusuki et al. (5) have reported the TiO_2 assisted photo-oxidation of toluene in air, and found that 80 ppm of this reactant could be completely oxidized to CO_2, with formation of less than 1 ppm of benzaldehyde as the only detectable intermediate at a toluene conversion of approximately 80%. The amount of CO_2 formed for a 10 minute reaction time was found to increase linearly with percent relative humidity.

We report here steady-state data of m-xylene heterogeneous photo-oxidation (Table 1). The integrated L-H rate form accounts again for reactant disappearance (Figure 9), with K=0.00659 m^3/mg and k=1.30 g/mg being the kinetics parameter values. No reaction intermediates were detected by GC-FID. In the hypothetical case of formation of an aldehyde derivative at 1% of total reactant, like the benzaldehyde found by Ibusuki, this low amount would probably not have been detected.

A study of water vapor influence on m-xylene photo-oxidation reaction rate (figure 10) showed that there is an increase in rate with the initial increase of water content up to values of 1000-1500 mg/m^3. For higher water concentrations the reaction rate is inhibited, as indicated by the approximately inverse variation of rate for feed water vapor content above 3000 mg/m^3.

DISCUSSION

Under illumination of wavelengths < 370 nm, the valence band electrons of the TiO_2 can be excited to the conduction band, creating highly reactive electron-hole pairs which, after migration to the solid surface, can be trapped at different sites. The nature of these sites and the trapping mechanisms are yet a subject of discussion among researchers, but it seems quite well accepted that the final electron traps for vapor-solid photocatalysis are the oxygen species on the surface, with O_2^- or O^- being the products of that electron transfer, as indicated for example by the dependence of photoconductance on P_{O2} (22). Munuera (23) sugested that Ti^{4+} centers capture the conduction band electrons and the Ti^{3+} ions formed are responsible for oxygen photoadsorption. At the same time the photogenerated holes are trapped by hydroxyl ions or water on the surface, producing hydroxyl redicals. The following mechanism represents these initial reaction steps:

$$TiO_2 + h\nu \longrightarrow h^+ + e^-$$

$$h^+ + OH^- \longrightarrow OH\cdot$$

$$Ti^{4+} + e^- \longrightarrow Ti^{3+}$$

and $$Ti^{3+} + O_{2ads} \longrightarrow Ti^{4+} + O^-_{2ads}$$

or $$O_{2ads} \longrightarrow 2\ O_{ads}$$

$$Ti^{3+} + O_{ads} \longrightarrow Ti^{4+} + O^-_{ads}$$

This mechanism of charge trapping is supported by the observation that oxygen photoadsorption is increased with increased surface hydroxyl concentration, and does not take place on completely *dry* surfaces (18). The hole trapping by the

hydroxyl species prevents electron-hole recombination at the surface, thus allowing oxygen chemisorption and electron-transfer. Two types of hydroxyls, differing by the strength of the bond formed with the surface, have been found by IR studies (24,25), isotopic exchange and adsorption-desorption measurements (18). The less strongly bound hydroxyls are easily removed at modest temperatures, and this occurence does not affect the photocatalytic activity. In contrast, removal of the strongly bound hydroxyls results in complete activity loss (18). For these reasons, the hydroxyl radical derived from water is widely accepted as a primary oxidant in heterogeneous photocatalysis; in vapor-solid photocatalysis, direct hole oxidation of adsorbed reactant is also a possibility.

The mechanism of hydroxyl radical attack depends on the type of organic involved. Blake and Griffin (7) found that butyraldehyde and butene were formed from 1-butanol in a constant ratio under many different experimental conditions. They concluded that these products are formed by parallel reactions from the same intermediate. A suggested mechanism involved hydroxyl radical attack of adsorbed alcohol to give aldehyde and water, both subsequently desorbing, or a dehydration leading to desorption of water and olefin. Under our steady-state conditions, the hydroxyl-alcohol reaction is completely dominant, and only a trace second product is observed.

In acetone photo-oxidation, we detected no reaction intermediate; prior studies at much higher partial pressures have reported trace H_2CO formation, and it seems probable that the only other possibles intermediates are HCOOH and CH_3COOH. The photocatalyzed decompositions of these last two gaseous reactants into CO_2 and water have been already demostrated (26), and as shown in Table 1,

H_2CO is rapidly destroyed under photocatalytic conditions. Thus, our trace concentrations of acetone studied appear to be cleanly converted to CO_2 and water by means of heterogeneous photocatalysis over TiO_2.

Widely differing rate influences of water have been reported for different photocatalyzed vapor phase oxidations. Dibble and Raupp found the rate of trichloroethylene oxidation to be zero order in water for H_2O mole fractions below 10^{-3}, and to become strongly inhibitory with a -3 order rate dependence for water mole fractions between $5 \cdot 10^{-3}$ and $5 \cdot 10^{-2}$. In contrast, Ibusuki et al. (5) found that the photocatalyzed oxidation rate of trace toluene (80 ppm) in air was enhanced by water vapor, increasing almost linearly with water vapor content between 0 and 60 % relative humidity. In the present study, water vapor feed concentrations of 250 to 10000 mg/m^3 (0.6 to 25 % of relative humidity) are clearly inhibitory for acetone photo-oxidation, but do not affect the rate of 1-butanol reaction. This behaviour may be explained in terms of adsorption competition: acetone appears to be less strongly adsorbed onto the TiO_2 than 1-butanol, thus water may displace surface adsorbed acetone but not 1-butanol, and thereby inhibit photocatalyzed oxidation of the former but not the latter. The variable role of water on m-xylene photo-oxidation may follow that of TCE (6), where trace water was required for activity, but excess water was inhibitory. The strong adsorption of 1-butanol would explain also the detection of butyraldehyde as a desorbed intermediate. Negligible levels of conversion of this aldehyde byproduct were accomplished with 1-butanol still present, presumably because of displacement by competitive adsorption. In the acetone case, any FID detectable intermediates formed were not forced to leave the surface due to adsorption competition with the reactant, and their photocatalytic decomposition could occur

before desorption took place.

The existence of photocatalyst deactivation after photo-oxidation of alcohols has been reported previously by Cumningham et al. (27). These authors examined the photocatalytic oxidation of 2-butanol and 2-propanol over illuminated TiO_2 and ZnO and used much higher pressures of alcohol, e.g. 8 mm Hg of 2-butanol (about 25000 ppm). Deactivation profiles seen were similar to ours found at 160-260 mg/m^3 (about 120-200 ppm). The authors suggested that CO_2 product bound to the surface could block some reactive sites, leading to surface deactivation. Rate data with CO_2 added over ZnO was presented which was consistent with this hypothesis, but no data or reference to TiO_2 was offered.

Since all oxidations produce CO_2 but deactivation has only been noted for alcohols, a more likely explanation of this deactivation peculiar to alcohols is that some other reaction product is able to deactivate or block some sites. This adsorbed material is oxidizable under appropriate conditions, since our catalyst may be regenerated photocatalytically in pure air as noted. Also, the achievement of steady-state conditions within every illumination period indicates that the deactivation agent eventually disappears at the same rate as its formation.

The amounts of intermediate products that remain adsorbed onto the catalyst after illumination could be responsible for the deactivation reported after every dark period. If one intermediate was sufficiently reactive, the deactivating species could be formed under dark conditions. Blake and Griffin (7) proposed an interesting mechanism of photo-oxidation for 1-butanol which involved not only butyraldehyde and butene formation as discussed above but also the formation of

butanoic acid from butyraldehyde, in order to rationalize tha slow appearance of carboxylate IR bands. Because butanoic acid is expected to be strongly adsorbed onto the TiO_2 surface and because any adsorbed aldehyde may be quite reactive, the acid may be responsible for our slow catalyst deactivation, which is enhanced during each dark period by the dark oxidation of the remaining butyraldehyde. The regeneration could then be due to photocatalyzed decarboxylation, by direct hole attack on adsorbed carboxylate to give

$$RCOO^-(ads) + h^+ \longrightarrow RCOO\cdot(ads) \longrightarrow CO_2 + R \longrightarrow \text{products}$$

A different, continuous deactivation of catalyst was found when no water vapor was present in the gas feed. This continuous loss of activity is reminiscent of the observation by Dibble and Raupp (6) that, for trichloroethylene photocatalyzed oxidation, a water-free fed led ultimately to a complete loss of activity, whereas as the presence of trace water allowed indefinite maintenance of activity. In the absence of feed water, their catalyst surface presumably became exhausted of the hydroxyls groups required for hole trapping and the formation of hydroxyl radicals that are responsible for organic oxidationt. A potentially important difference is that water itself is a reactant for TCE destruction but a product of photocatalyzed oxidation of less substituted hydrocarbons.

CONCLUSIONS

Trace (1-260 mg/m^3) concentrations of acetone, 1-butanol, butyraldehyde, formaldehyde, and m-xylene in air were succesfully diminished by degradation (oxidation) in the presence of near-UV illuminated TiO_2 anatase powder. Integral conversion rate data from single component runs provided kinetics parameters for a Langmuir-Hinshelwood rate expression. No reactions intermediates of acetone photo-oxidation were detected; we assume that acetone was eventually converted to CO_2. Butyraldehyde was the main product of 1-butanol photo-oxidation, but no 1-butene was detected, in contrast to prior literature for reaction at much higher 1-butanol levels. A secondary trace peak from 1-butanol oxidation also appeared during butyraldehyde photo-oxidation; attempts to identify that product were unsuccesful. Formaldehyde photo-oxidation at levels of 6-90 ppm were carried out with no products detected via flame ionization.

Catalyst deactivation was noticed when photo-oxidizing 1-butanol or butyraldehyde; it appears due to adsorbed species formed through light or dark reactions between one or more intermediate products of photo-oxidation. The activity was recovered by illuminating the TiO_2 photocatalyst in presence of pure air, indicating the oxidizable nature of the deactivating species.

The ability of the catalyst to react an aldehyde, an alcohol and a ketone at trace levels, along with prior literature demostrating the conversion of simple alkanes, trichloroethylene and toluene and several odor-associated compounds, indicates that all major classes of trace oxidizable air contaminants may be candidates for photocatalytic destruction.

Water inhibits acetone conversion but has no influence on 1-butanol rate. It appears to activate and inhibit m-xylene photo-oxidation at low and higher vapor levels, respectively. Since literature results indicate that toluene total oxidation is enhanced and TCE destruction is inhibited by air humidification, the multiple roles of water in gas-solid photocatalysis deserve further exploration.

ACKNOWLEDGEMENTS

This work was supported by NASA Research Grant NAG 2-684 (Reactor, chemicals and analysis) and by the Ministerio de Educación y Ciencia of Spain (Post-Doctoral fellowship for J. Peral). We acknowledge helpful comments from NASA's Advanced Life Support Technology Program, Office of Aeronautics, Exploration and Technology (Program Manager: Ms. Peggy L. Evanich; Technical Monitor: Dr. Edwin L. Force). A preliminary version of this paper was presented at the August 1991 AIChE meeting in Pittsburgh, PA.

APPENDIX

Mass transfer influence unimportant. Consider an illustrative run condition:

Butanol feed rate = 11.3 μg/min

Air feed rate = 0.0875 g/min

Butanol feed concentration ($C_{i,B}$) = $1.611 \cdot 10^{-7}$ g/cm^3

Butanol reaction rate (J_i) = 2.78 μg/min = $4.63 \cdot 10^{-8}$ g/s

Superficial velocity = 22.3 cm/min

Superficial flow cross section = 3.14 cm^2

Superficial mass velocity (G) = $4.6 \cdot 10^{-4}$ g/cm$^2 \cdot$s

Reynolds number (Re) = $D_p \cdot G/\mu$ = 0.135

Schmidt number (Sc) = $\mu/\rho \cdot \mathcal{D}$ = 0.136

Packed bed j factor correlation (10):

$$\epsilon_B j_D = \frac{1.09}{Re^{2/3}}$$

with ϵ_B = 0.4, j_D = 10.35

External mass transfer coefficient $K_{c,i}$:

$$K_{c,i} = \frac{G}{\rho} Sc^{-\frac{2}{3}} j_D = \frac{J_i}{C_{i,B} - C_{i,s}}$$

Illuminated mass is 3.14 cm^2 · $4.5 \cdot 10^{-4}$ cm ·3.8 g/cm^3 ≈ $5.4 \cdot 10^{-3}$ g

A_c = Illuminated surface area is $5.4 \cdot 10^{-3}$ g · $5 \cdot 10^5$ cm^2/g = 2.68 cm^2

$$\frac{J_i}{A_c} = 1.72 \cdot 10^{-11} \frac{g}{cm^2 s}$$

$$C_{i,B}-C_{i,s}=\frac{J_i\rho}{G\cdot Sc^{-\frac{2}{3}}j_D}=1.19\cdot10^{-12}\frac{g}{cm^2}$$

$$C_{i,s}=1.61\cdot10^{-7}\frac{g}{cm^3}$$

$$\frac{C_{i,B}-C_{i,s}}{C_{i,B}}=7\cdot10^{-6}=7\cdot10^{-4}\%$$

Bulk and near surface gas phase concentrations of 1-butanol are virtually identical. No mass transfer influence is present, and data thus represent intrinsic chemical kinetics of surface reaction.

REFERENCES

1. Ollis, D.F., Environ. Sci. Technol., 19, 480 (1985).
2. Ollis, D.F., Pelizzetti, E., Serpone, N., In *Photocatalysis: Fundamentals and Applications*, Serpone, N.; Pelizzetti, E., Eds., Wiley: New York, 1989; pp. 604-37.
3. Ollis, D.F., Pelizzetti, E., Serpone, N., Environ. Sci. Technol., 25, 1523 (1991).
4. Courbon, H., Formenti, M., Juillet, F., Lisachenko, A.A., Martin, J., Teichner, S.J., Kinet. Catal., 14, 84 (1973).
5. Ibusuki, T., Takeuchi, K., Atmospheric Environtment 20, 1711 (1986).
6. Dibble, L.A., Raupp, G.B., Catal. Letters 4, 345 (1990).
7. Blake, N.R., Griffin, G.L., J. Phys. Chem. 92, 5698 (1988).
8. Bickley, R.I., Munuera, G., Stone, F.S., J. Catal. 31, 389(1973).
9. Suzuki, K., Satoh, S., Yoshida, T., Oenki Kagaku 59, 521(1991).
10. NIOSH Manual of Analytical Methods, 2nd Ed., Vol. 7, Method P&CAM 354, DHHS (NIOSH) Pub. No. 82-100 (Aug. 1981).
11. Hill, C.G., "An Introduction to Chemical Engineering Kinetics and Reactor Design", p. 475, John Wiley, New York, 1977.
12. Djeghri, N., Teichner, S.J., J. Catal. 62, 99 (1980).
13. Formenti, M., Juillet, F., Meriadeau, P., Teichner, S.J., Chem. Technol. 1, 680(1971).
14. Egerton, T.A., King, C.J., J. Oil Col. Chem. Assoc. 62, 386 (1979).
15. Okamoto, K., Ysamamoto, Y., Taneka, H., Itaya, A., Bull. Chem. Soc. Japan 58, 2023 (1985).
16. D'Oleivera, J., Al-Sayyed, G., Pichat, P., Environmental Science and Technol. 24, 990 (1990).

17. Pruden, A.L., Ollis, D.F., J. Catal., 82, 404 (1983).

18. Bickley, R.I., Stone, F.S., J. Catal 31, 389 (1973).

19. Cunningham, J., Hodnett, B.K., Ilyas, M., Tobin, J., Leahy, E.L., Faraday Discuss. Chem. Soc. 72, 283 (1981).

20. Boonstra, A.H., Mutsaers, C.A.H.A., J. Phys. Chem., 79, 1694 (1975).

21. Plog, B.A., Ed., "Fundamentals of Industrial Hygiene", National Safety Council, 1988, pag. 775.

22. Pitchat, P., Herrmann, J., Courbon, H., Disdier, J., Mozzanega, M., Can. J. Chem. Eng. 60, 27 (1982).

23. Munuera, G, Rives-Arnau, V., Saucedo, A., J. Chem. Soc. Faraday Trans.1 75, 736 (1979).

24. Primet, M., Pichat, P., Mathieu, J. Phys. Chem. 75, 1216 (1971).

25. Primet, M., Pichat, P., Mathieu, J. Phys. Chem. 75, 1221 (1971).

26. Sato, S., J. Phys. Chem. 87, 3531 (1983).

27. Cunningham, J. Hodnett, B.K., J. Chem. Soc. Faraday Trans. 1 77, 2777 (1981).

FIGURE AND TABLE CAPTIONS

Figure 1. Experimental system.

Figure 2. Plot of $(C-C_0)^{-1} \cdot \ln(C/C^0)$ vs. $(C-C_0)^{-1}$ for acetone data in table 1. $I_a = 3.5 \cdot 10^{-7}$ Eins/cm_2·min (200 W high pressure Hg-Xe lamp); T=22-24 °C.

Figure 3. Reaction rate of acetone photo-oxidation and quantum yield vs. irradiance. $[Acetone]_0$=160 mg/m^3; T=22-24 °C. Reaction rate and irradiance units are μg/cm^2·min and Einstein/cm^2·min, respectively.

Figure 4. Inverse of reaction rate of acetone photo-oxidation vs. water concentration in the gas phase. $[Acetone]_0$=200 mg/m^3; T=22-24 °C. 200 W high pressure Hg-Xe lamp. Reaction rate and water concentration units are mg/cm^2·min and mg/m^3, respectively.

Figure 5. Plot of $(C-C_0)^{-1} \cdot \ln(C/C^0)$ vs. $(C-C_0)^{-1}$ for 1-butanol data in table 1. $I_a = 5.0 \cdot 10^{-7}$ Eins/cm^2·min (100 W blacklight); T=22-24 °C.

Figure 6. Reaction rate of 1-butanol photo-oxidation and butyraldehyde formation vs. water concentration in the gas phase. $I_a = 5.0 \cdot 10^{-7}$ Eins/cm^2·min (100 W blacklight); T=22-24 °C.

Figure 7. Deactivation of photo-steady-state for 1-butanol conversions (see text for details). $[Butanol]_0$=260 mg/m^3; $I_a = 5.0 \cdot 10^{-7}$ Eins/cm^2·min; T=22-24 °C.

Figure 8. Plot of $(C-C_0)^{-1} \cdot \ln(C/C^0)$ vs. $(C-C_0)^{-1}$ for butyraldehyde data in table 1. $I_a=5.0 \cdot 10^{-7}$ Eins/cm^2·min (100 W blacklight); T=22-24 °C.

Figure 9. Plot of $(C-C_0)^{-1} \cdot \ln(C/C^0)$ vs. $(C-C_0)^{-1}$ for m-xylene data in table 1. $I_a=5.0 \cdot 10^{-7}$ Eins/cm^2·min (100 W blacklight); T=22-24 °C.

Figure 10. Reaction rate of m-xylene photo-oxidation vs. water concentration in the gas phase. $I_a=5.0 \cdot 10^{-7}$ Eins/cm^2·min (100 W blacklight); T=22-24 °C.

Table 1. Reactor feed and exhaust steady-state concentrations of acetone, 1-butanol, butyraldehyde and m-xylene under photocatalytic conditions. Acetone data was obtained by using a 200 W Hg-Xe lamp. 1-Butanol, m-xylene and formaldehyde data were obtained with a 100 W blacklight. Concentrations are expressed in mg/m^3. Pyrex filter in all runs.

Table 2. Catalyst deactivation and activity recovery. [Water]=1000 mg/m^3; $I_a=5.0 \cdot 10^{-7}$ Eins/cm^2·min; T=22-24 °C.

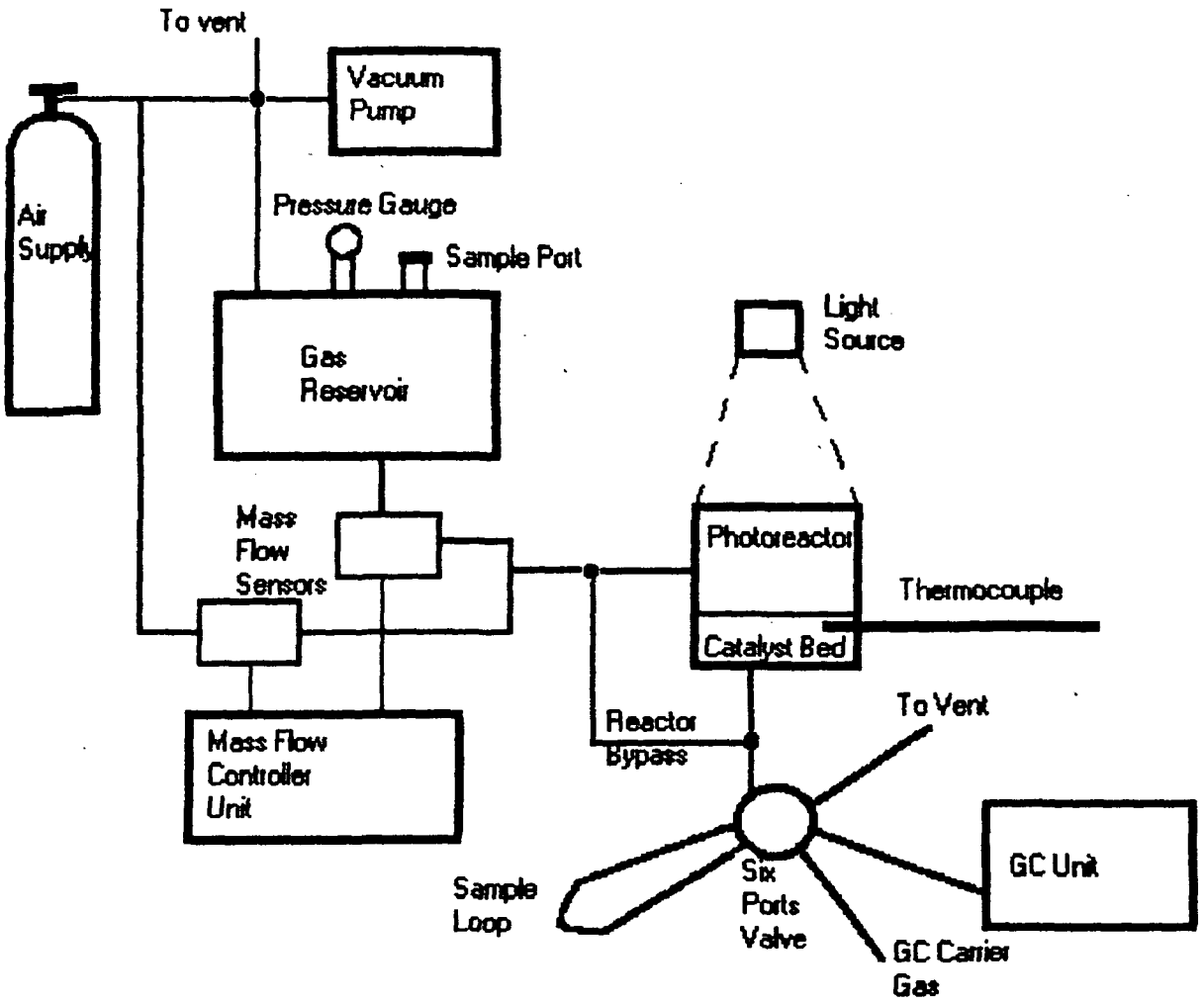
To vent
Vacuum Pump
Air Supply
Pressure Gauge
Sample Port
Gas Reservoir
Light Source
Mass Flow Sensors
Photoreactor
Thermocouple
Catalyst Bed
Reactor Bypass
To Vent
Mass Flow Controller Unit
GC Unit
Sample Loop
Six Ports Valve
GC Carrier Gas

Fig. 1

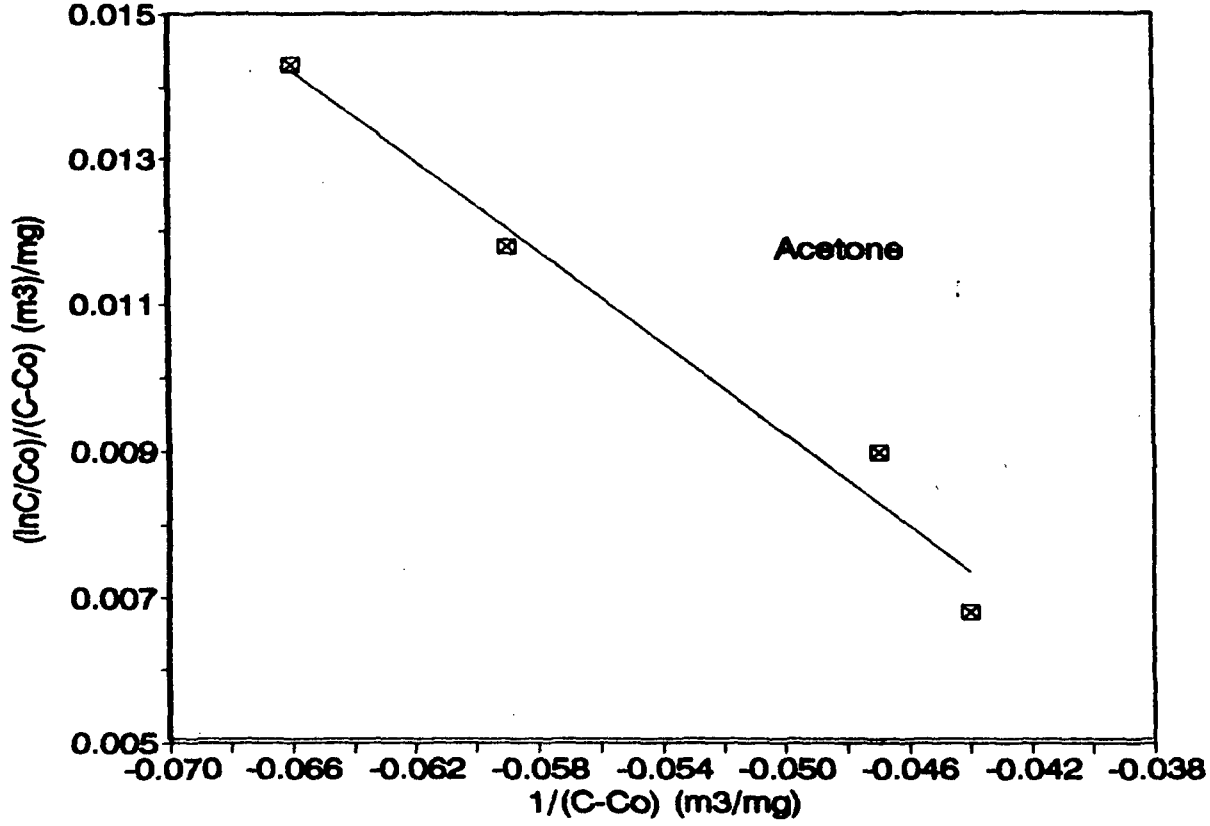
0.015
0.013
0.011
0.009
0.007
0.005
(lnC/Co)/(C-Co) (m3/mg)
Acetone
-0.070
-0.066
-0.062
-0.058
-0.054
-0.050
-0.046
-0.042
-0.038
1/(C-Co) (m3/mg)

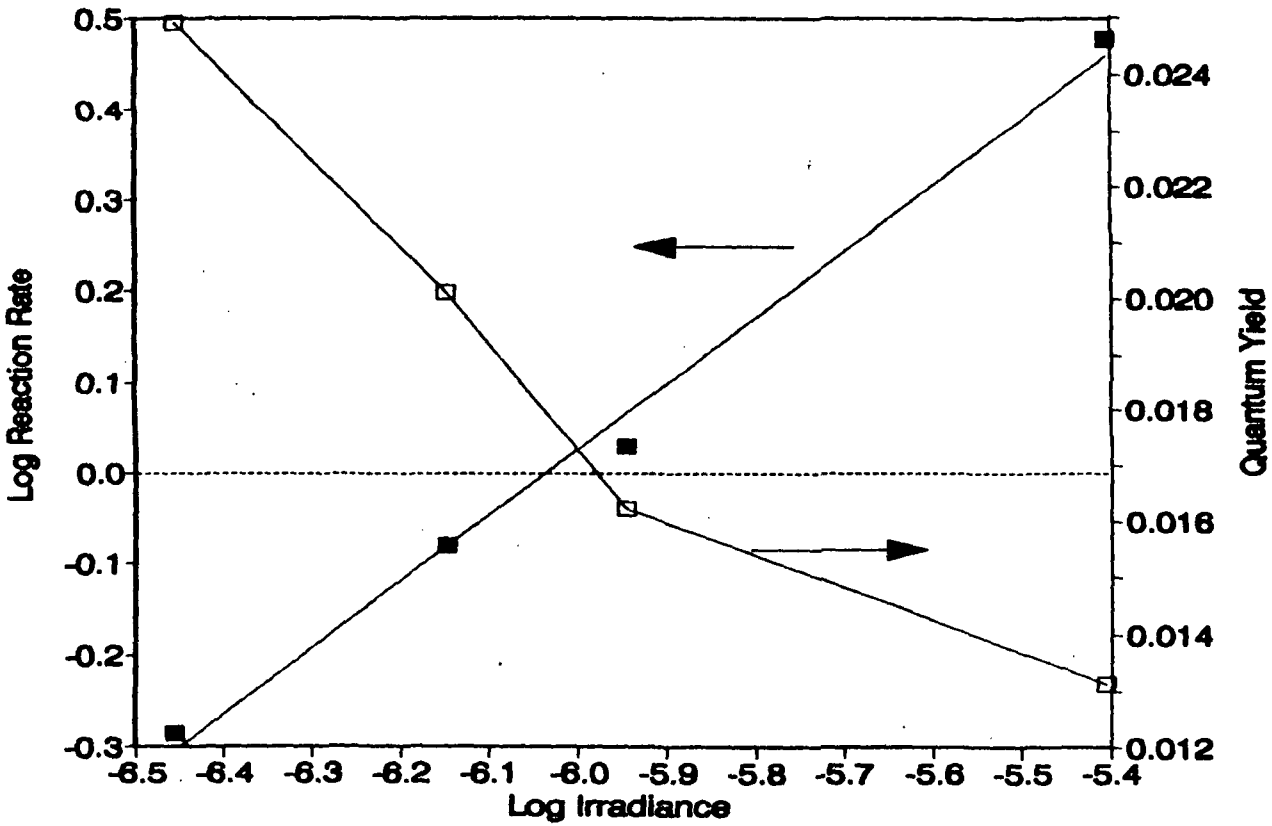
0.5
0.4
0.3
0.2
0.1
0.0
-0.1
-0.2
-0.3
Log Reaction Rate
0.024
0.022
0.020
0.018
0.016
0.014
0.012
Quantum Yield
-6.5
-6.4
-6.3
-6.2
-6.1
-6.0
-5.9
-5.8
-5.7
-5.6
-5.5
-5.4
Log Irradiance

Fig 3

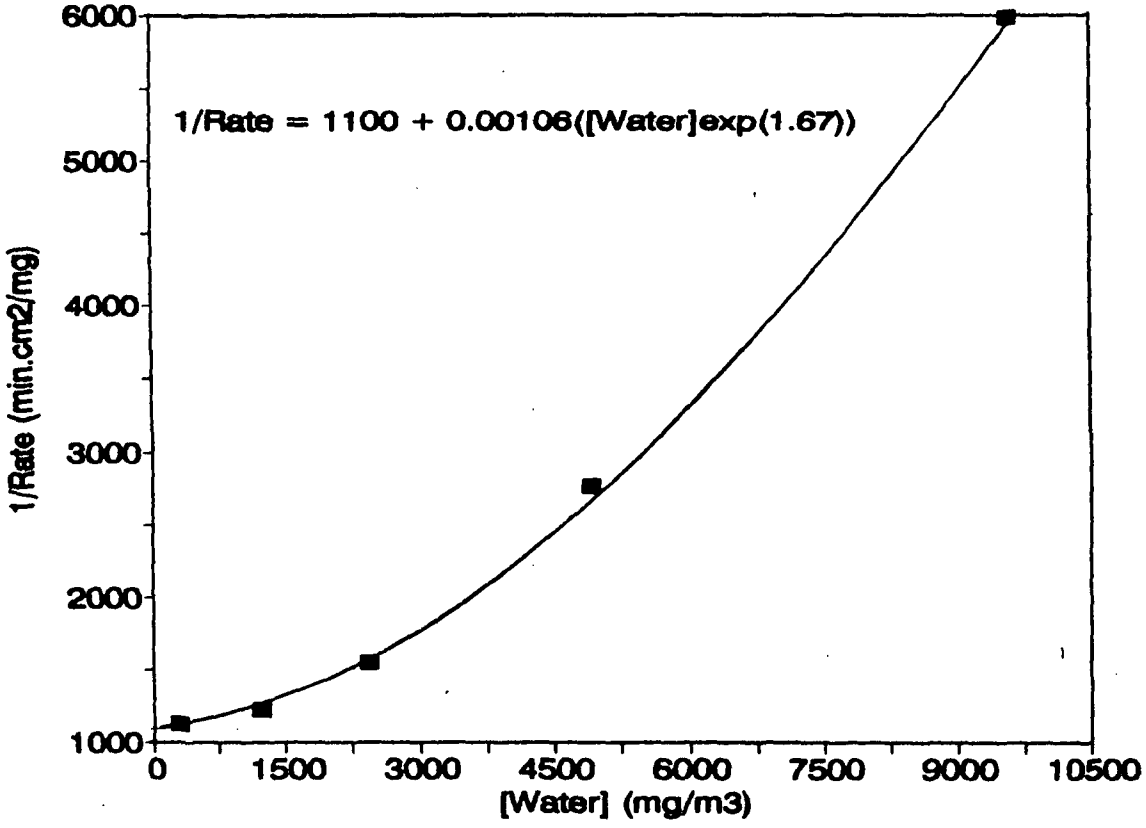
1/Rate = 1100 + 0.00106([Water]exp(1.67))
6000
5000
4000
3000
2000
1000
1/Rate (min.cm2/mg)
0
1500
3000
4500
6000
7500
9000
10500
[Water] (mg/m3)

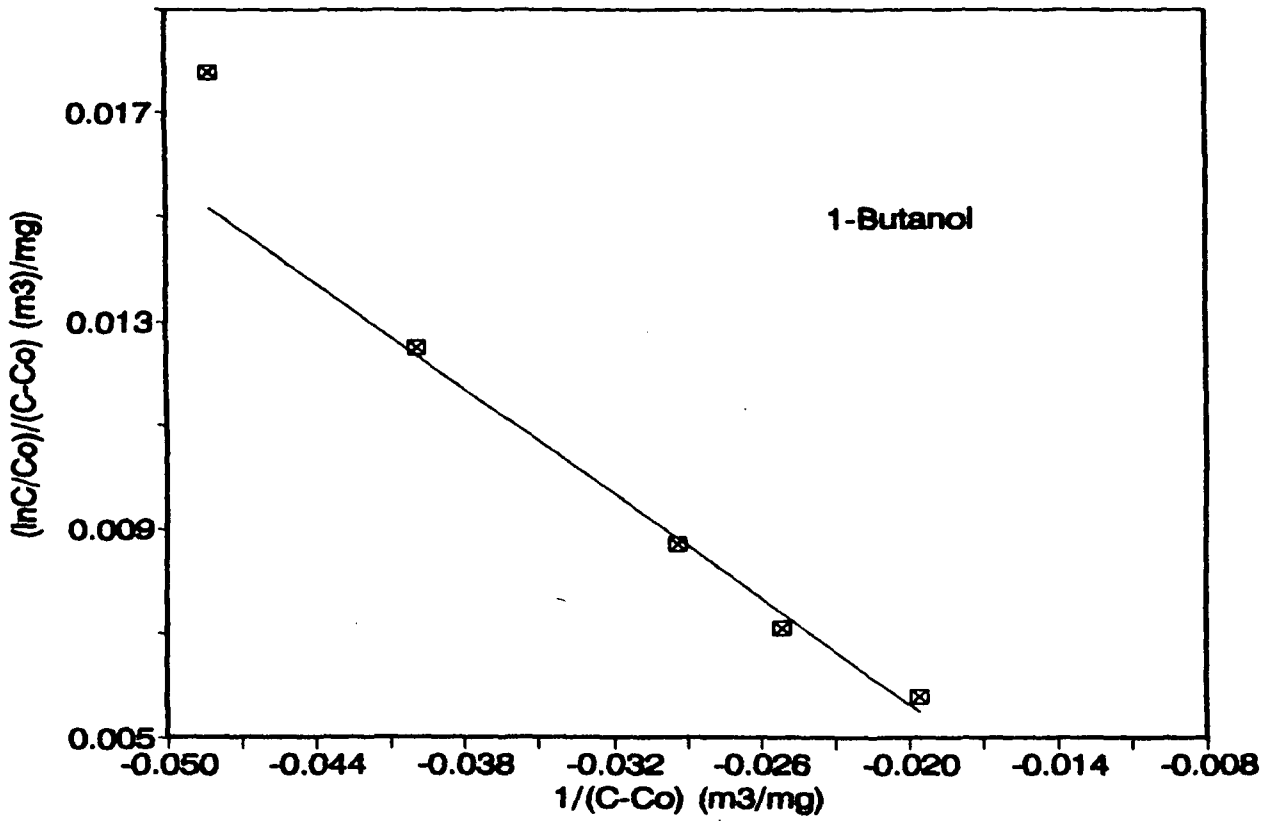
1-Butanol
0.017
0.013
0.009
0.005
(lnC/Co)/(C-Co) (m3)/mg
-0.050
-0.044
-0.038
-0.032
-0.026
-0.020
-0.014
-0.008
1/(C-Co) (m3/mg)

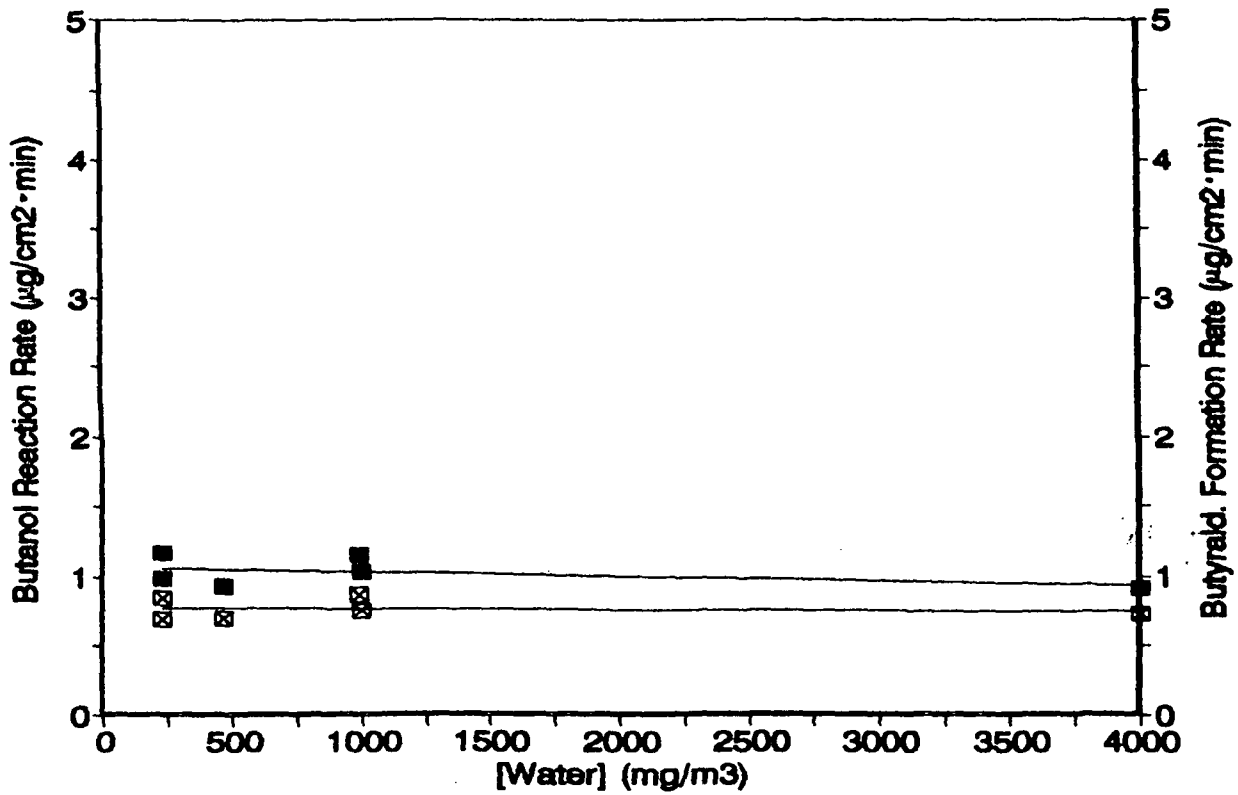
Butanol Reaction Rate (µg/cm2·min)
Butyrald. Formation Rate (µg/cm2·min)
[Water] (mg/m3)
0
1
2
3
4
5
0
500
1000
1500
2000
2500
3000
3500
4000

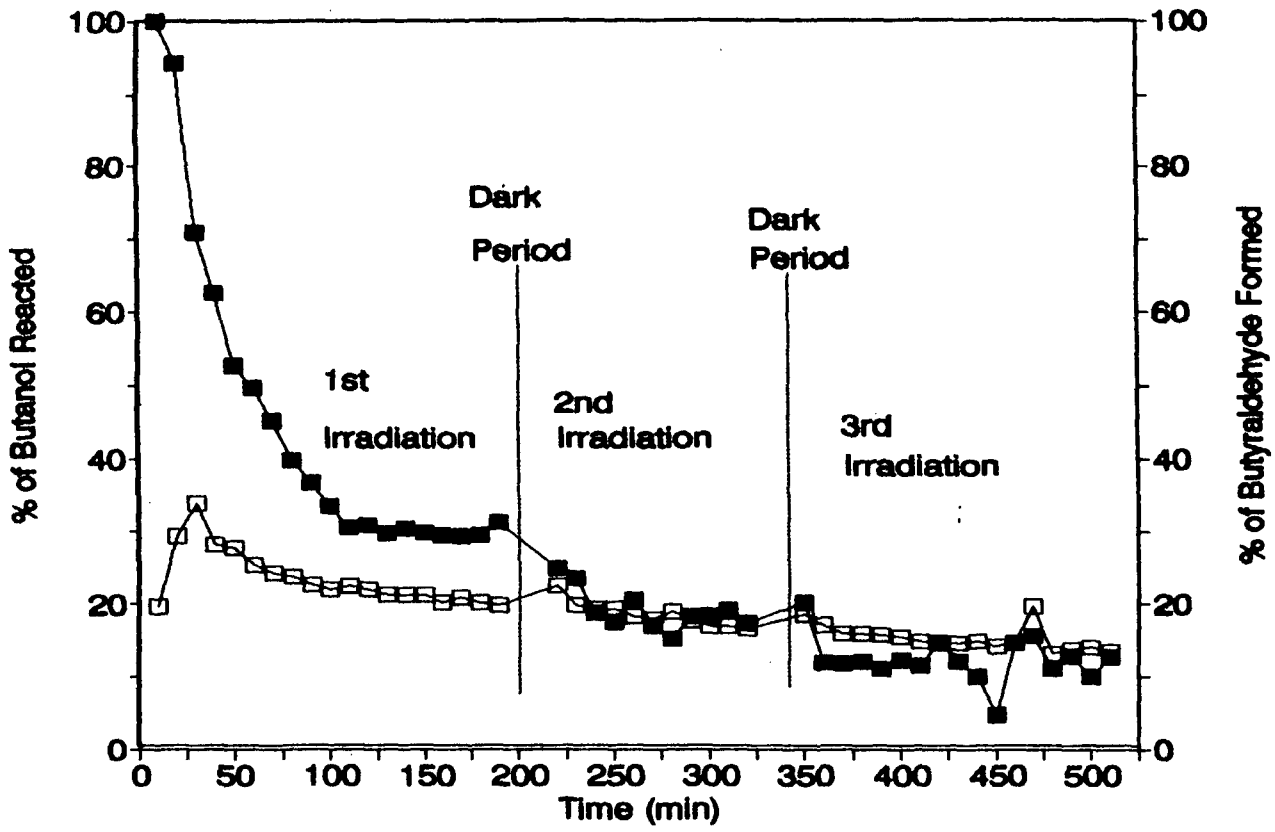
% of Butanol Reacted
% of Butyraldehyde Formed
Time (min)
Dark Period
Dark Period
1st Irradiation
2nd Irradiation
3rd Irradiation
0
20
40
60
80
100
0
50
100
150
200
250
300
350
400
450
500

Fig. 7

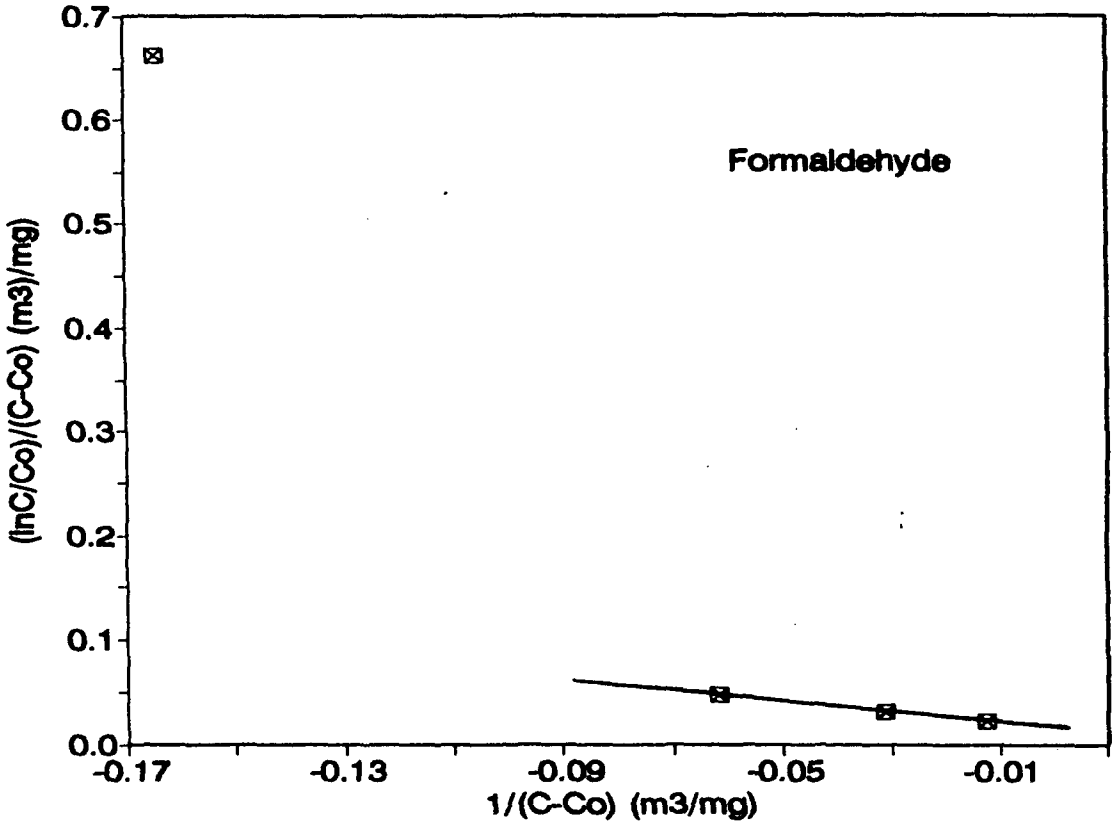
Formaldehyde
(lnC/Co)/(C-Co) (m3/mg)
0.7
0.6
0.5
0.4
0.3
0.2
0.1
0.0
-0.17
-0.13
-0.09
-0.05
-0.01
1/(C-Co) (m3/mg)

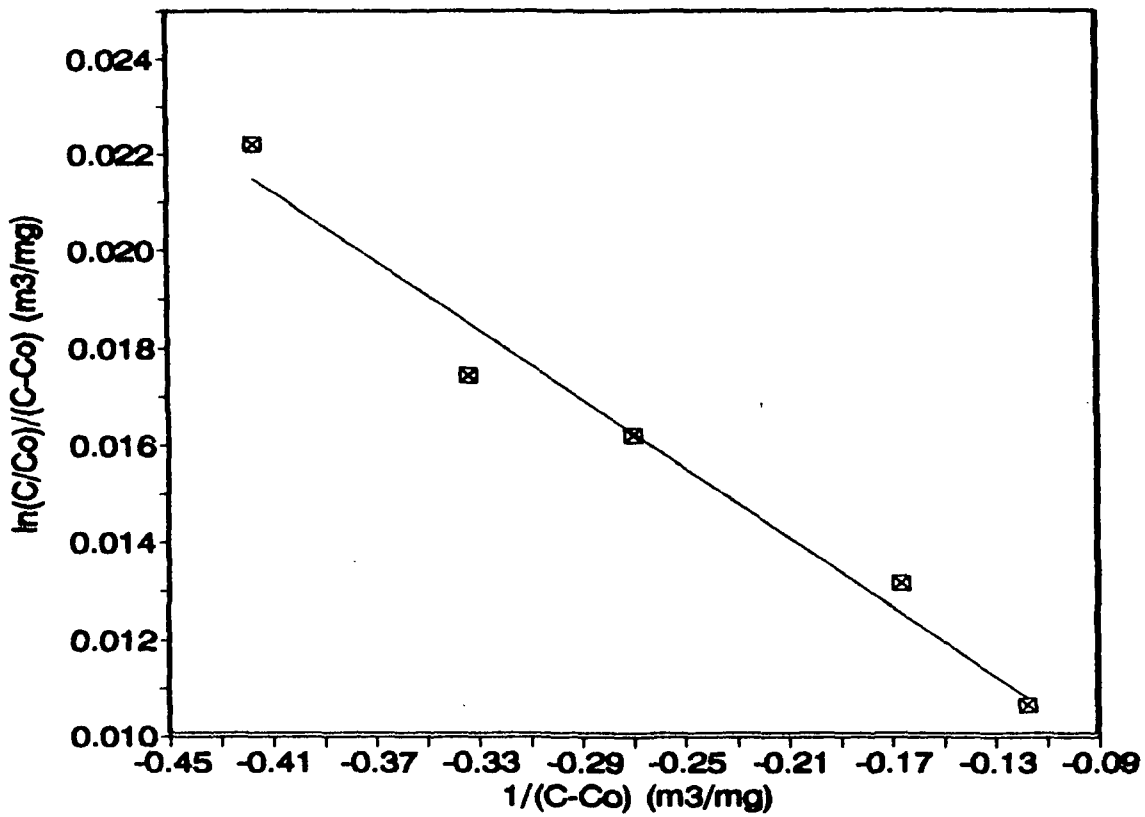
0.024
0.022
0.020
0.018
0.016
0.014
0.012
0.010
ln(C/Co)/(C-Co) (m3/mg)
-0.45
-0.41
-0.37
-0.33
-0.29
-0.25
-0.21
-0.17
-0.13
-0.09
1/(C-Co) (m3/mg)

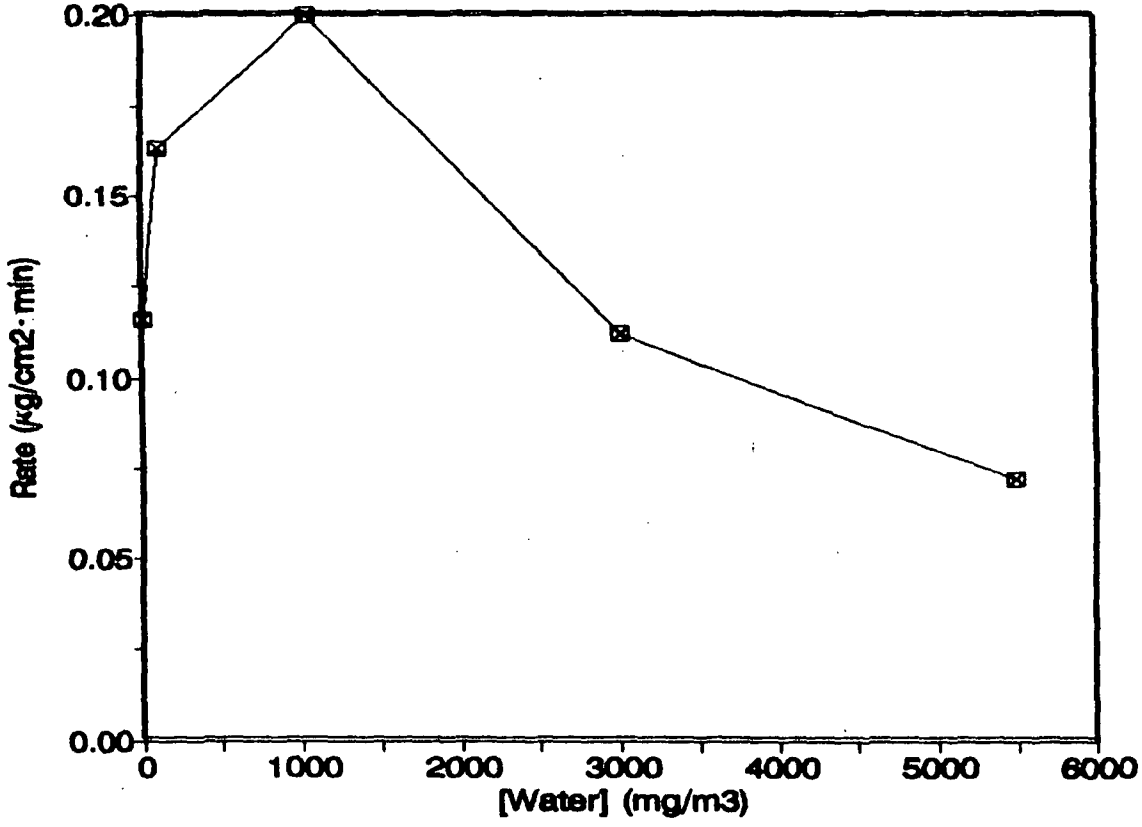
0.20
0.15
0.10
0.05
0.00
Rate (kg/cm2·min)
0
1000
2000
3000
4000
5000
6000
[Water] (mg/m3)

Acetone		1-Butanol		Formaldehyde		m-Xylene	
C_0	C	C_0	C	C_0	C	C_0	C
77.6	62.5	67	46.3	6.2	0.1	98.3	89.7
92.2	75.5	93.2	68.2	30.1	13.9	79	73.0
123.7	102.1	132.3	98.3	50.3	18.2	63.5	59.9
158.7	136	161.1	121.4	96.1	15.7	58.8	55.8
		202	150			46.2	43.8

Table 1

Day	Catalyst Pretreatment Conditions	Butanol (mg/m^3)	Rate Butanol Oxidation ($\mu g/cm^2 \cdot min$)	Rate Butyral Formation ($\mu g/cm^2 \cdot min$)
1	Fresh Catalyst	132	2.38	1.19
19	After several runs	125.8	1.48	1.20
22	Fresh air flow during 90 min(dark)	141	1.15	0.87
26	Fresh air flow overnight (dark)	150	0.92	0.70
39	Fresh air flow overnight (light)	151	1.88	1.23
67	Fresh air flow (74 °C, dark)	129.1	0.34	0.29
68	Fresh air flow overnight (light)	132.3	0.42	0.94
93	Fresh air flow (49 °C, dark)	126	0.56	0.29